Journal of Interventional Cardiac Electrophysiology 1999;3:213–224

Electrical Impedance Properties of Normal and Chronically Infarcted Left Ventricular Myocardium

David Schwartzman[1], Isaac Chang[2], John J. Michele[1], Mark S. Mirotznik[3], and Kenneth R. Foster[2]

[1]Cardiovascular Research Laboratory, Philadelphia Heart Institute; [2]Department of Bioengineering, University of Pennsylvania; [3]Department of Electrical Engineering, Catholic University of America

Abstract. **Background: Previous reports have disclosed that a significant difference exists between the electrical impedance properties of healthy and chronically infarcted ventricular myocardium.**

Purpose: **To assess the potential utility of electrical impedance as the basis for mapping in chronically infarcted left ventricular myocardium. Specifically: (1) to delineate electrical impedance properties of healthy and chronically infarcted ventricular myocardium, with special emphasis on the infarction border zone; (2) to correlate impedance properties with tissue histology; (3) to correlate impedance properties with electrogram amplitude and duration; (4) To demonstrate that endocardial impedance can be measured effectively *in vivo* using an electrode mounted on a catheter inserted percutaneously.**

Methods: **An ovine model of chronic left ventricular infarction was utilized. Sites of healthy myocardium, densely infarcted myocardium and the infarction border zone were investigated. Bulk impedance was measured *in vitro* using capacitor cell, four-electrode and unipolar techniques. Epicardial and endocardial impedances were measured *in vivo* using four-electrode and unipolar techniques. Impedance was measured at multiple frequencies. Electrographic amplitude, duration and amplitude/duration ratio were measured using bipolar electrograms during sinus rhythm. Quantitation of tissue content of myocytes, collagen, elastin and neurovascular elements was performed.**

Results: **Densely infarcted myocardial impedance was significantly lower than healthy myocardium. Impedance gradually decreased in the border zone transitioning between healthy myocardium and dense infarction. Decreasing impedance correlated with a decrease in tissue myocyte content. The magnitude of the difference in impedance between densely infarcted and healthy myocardium increased as the measurement frequency decreased. Healthy myocardium exhibited a marked frequency dependence in its impedance properties; this phenomenon was not observed in densely infarcted myocardium. There was a direct association between impedance and both electrogram amplitude and amplitude/duration ratio. There was an inverse association between impedance and electrogram duration. Endocardial impedance, measured *in vivo* using a electrode catheter inserted percutaneously, was demonstrated to distinguish between healthy and infarcted myocardium.**

Conclusions: **The electrical impedance properties of healthy and infarcted left ventricular myocardium differ markedly. The properties of the infarction border zone are intermediate between healthy and infarcted myocardium. Impedance may be a useful assay of cardiac tissue content and adaptable for cardiac mapping *in vivo*.**

Key Words. **impedance, cardiac mapping, infarction**

Introduction

Ventricular tachycardia occurring in the setting of chronic myocardial infarction often arises from areas of the border of an infarct scar in areas where a "barrier" histology is present [1]. The barrier is comprised of a multicellular layer of viable subendocardial myocytes sandwiched between dense layers of endocardial and intramural fibrosis. At the border, as the transition is made from densely infarcted to healthy myocardium, myocytes interdigitate with collagen bundles, and there is a gradual increase in the content of myocytes [2].

Previous investigation has shown that there are significant differences in the electrical impedance properties of normal and chronically densely infarcted myocardium [3,4]. However, these studies did not address the properties of the infarction border zone. In addition, they did not attempt to correlate impedance properties with tissue histology. Finally, no data has been published correlating impedance properties with local electrogram characteristics.

Supported in part by the Sidney Kimmel Cardiovascular Research Foundation of the Philadelphia Heart Institute. Supported in part by a Beginning Investigator Grant (DS) from the American Heart Association, Southeastern Pennsylvania Affiliate.

Address correspondence to: David Schwartzman, M.D., University of Pittsburgh Medical Center, Presbyterian University Hospital, B535, 200 Lothrop Street, Pittsburgh, PA 15213-2582. E-mail: dschwartzm@aol.com

Received 3 March, 1999; accepted 26 May 1999

We report the results of a multifaceted investigation, a goal of which was to assess the utility of electrical impedance for characterizing cardiac tissue content, specifically to characterize the properties of the infarction border zone. We utilized both *in vitro* and *in vivo* techniques. First, we assessed the impedance properties of densely infarcted and healthy myocardium *in vitro*, to confirm and extend the findings of previous investigators and to establish the validity of our infarction model. Second, we assessed endocardial impedance properties in the region of the infarction border zone *in vitro*, and performed a correlation with tissue histology. Third, we assessed epicardial impedance properties in the region of the infarction border zone *in vivo*, and correlated these properties with sinus rhythm electrogram characteristics. Fourth, we measured endocardial impedance in chronically infarcted ventricles *in vivo*, via an electrode catheter inserted percutaneously into a beating heart.

These data confirm that the electrical impedance properties of healthy and infarcted left ventricular myocardium differ markedly. The properties of the infarction border zone are intermediate between healthy and infarcted myocardium. Impedance properties are related to tissue histology. We propose that impedance might be a useful assay of cardiac tissue content, adaptable for cardiac mapping.

Methods

Ovine infarction model

Each protocol was approved by the Institutional Animal Care and Use Committee of the Presbyterian Medical Center of Philadelphia and was in compliance with the Guide for Care and Use of Laboratory Animals published by the National Institutes of Health, publication 78–83.

The model has been described previously [5]. Healthy adult male Dorsett sheep weighing 30–50 kilograms were utilized. The animals were pre-anesthetized with sodium thiopental (2.5%). After endotracheal intubation, anesthesia was maintained using isoflurane 2–4%. A left lateral thoracotomy was performed via the 4th intercostal space to expose the pericardium. The pericardium was incised and the left anterior descending coronary artery was isolated and ligated (suture) above the first diagonal branch. Incisions were then closed and the animals were observed initially at the surgical facility, and then on a biological farm. Subsequent studies were performed after sixty days. Litigation of the anterior descending coronary artery at this level resulted in dense infarction involving the anterior apical septum and apical free walls of the left ventricle. In the majority of animals dyskinesis was observed in this area, with no endocardial thrombus associated with the infarction in the chronic phase [5]. Although we did not perform programmed ventricular stimulation in these animals, previous investigators have reported that monomorphic ventricular tachycardia originating from the left ventricle can be reliably initiated and ventricular late potentials are common [6,7]. At pathological examination, the infarction border zone is characterized by a transition region extending over several millimeters from densely infarcted myocardium (almost exclusively collagen) to healthy myocardium, in which a barrier histology is present [5]. In this transition region, there is a broad area in which myocytes interdigitate with collagen bundles. Overlying the dense infarction and infarction border zone was fibrotic endocardium. Dense infarction extends to the epicardium (Fig. 1).

Impedance measurement techniques

1. Capacitor cell. A detailed review of this technique was presented by Schwan [8]. The technique is widely accepted as a method for measuring bulk electrical properties of tissue. Myocardial samples from parts of the left ventricle which were healthy antemortem as well as from densely infarcted areas were studied several hours after resection of the heart. The capacitor cell was comprised of two circular platinum electrodes (area 1 square centimeter each) which enclosed the tissue in a tubular lucite chamber (Fig. 2). The chamber was encased in a water jacket to maintain a constant temperature of 37 °C. A volume of myocardium filled the chamber so as to be in complete contact with both electrodes, with no current pathway outside the tissue. As this tissue volume was not constant between different specimens, the chamber volume was adjusted accordingly and a cell calibration constant was determined for each tissue sample tested. Current was then passed between the electrodes. The resultant potential difference arising between the electrodes was measured using an impedance analyzer (HP4192a, Hewlett-Packard, Inc.). The ratio of induced voltage to current is proportional to the tissue impedance. For each specimen, impedance values were obtained over a measurement frequency range of 1 kHz to 13 MHz ($\geq$5 points per frequency decade). Measurements were corrected for stray effects, including series inductance and shunt capacitance of the leads, using methods described by Schwan [8].

2. Four electrode. This technique had been previously validated and is widely accepted for the measurement of local tissue impedance (e.g., tissue in the region of contact with the measurement electrodes) [9]. The measurement instrument was comprised of four 27-gauge platinum pin electrodes equally spaced 2 millimeters apart (Fig. 3). Each electrode was insulated except for its distal 1.5 millimeters. A 10–20 microampere alternating current was passed between the outer two electrodes, and the resulting voltage gradient which developed between the inner two electrodes was measured using an impedance analyzer (Hewlett-Packard model 4192a). The ratio of induced

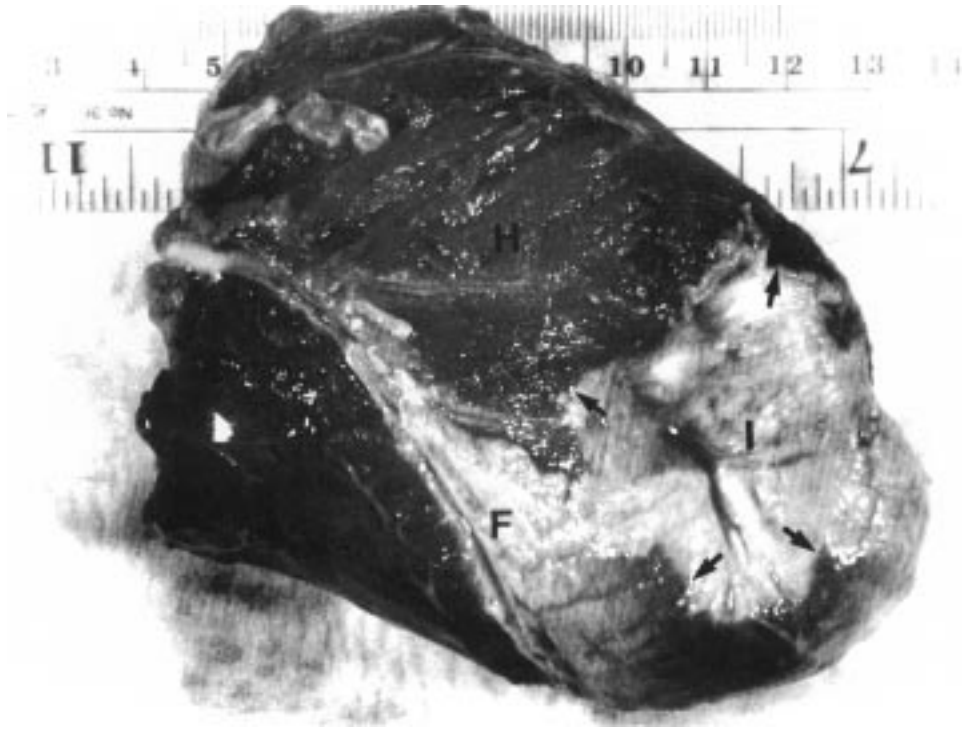

Fig. 1a. *Unmagnified gross specimen, anterior epicardial view of ventricles resected en bloc from a chronically infarcted animal. Pericardium has been stripped away, as has most of the epicardial fat with the exception of that in the interventricular groove (F). Dense infarction (I) appears white relative to areas of healthy myocardium (H). The infarction border (arrows) is generally discrete.*

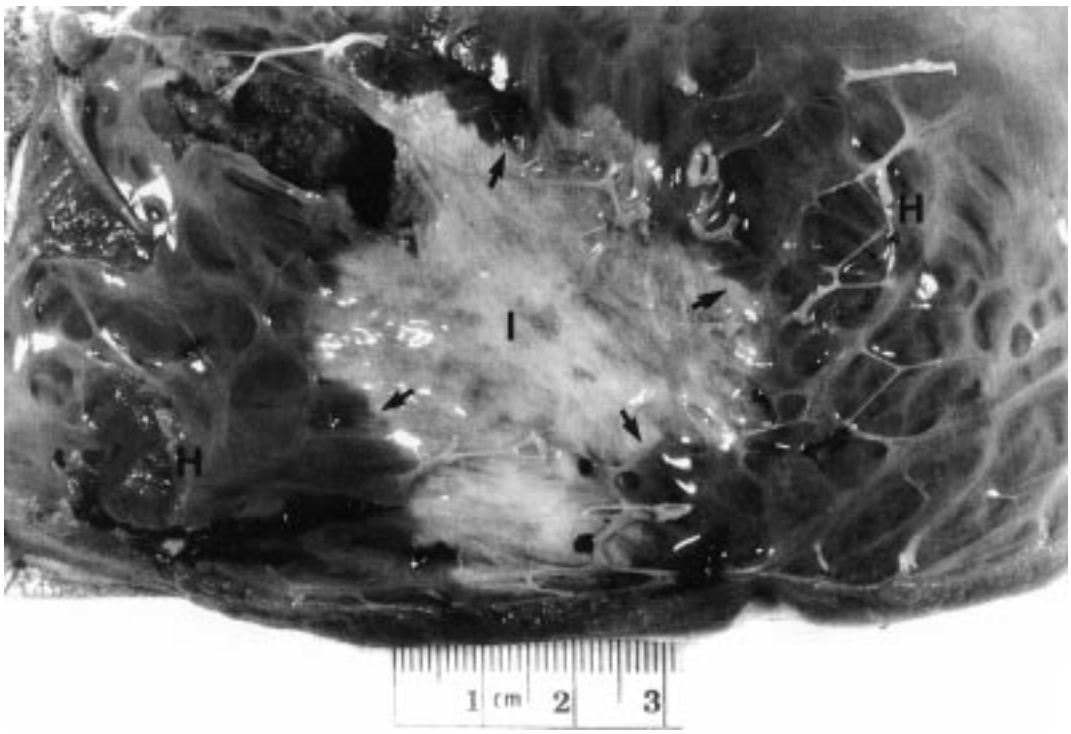

Fig. 1b. *Unmagnified gross specimen, endocardial view of left ventricle from a chronically infarcted animal. Dense infarction (I) appears white relative to areas of healthy myocardium (H). The infarction border (arrows) is generally discrete.*

Fig. 1c. *Magnified gross specimen of the infarction border, cross-sectional view. Dense infarction (I) appears white relative to areas of myocytes (H). At the infarct border, a layer of preserved subendocardial myocytes is sandwiched between a layer of endocardial fibrosis and a layer of intramural fibrosis (arrow).*

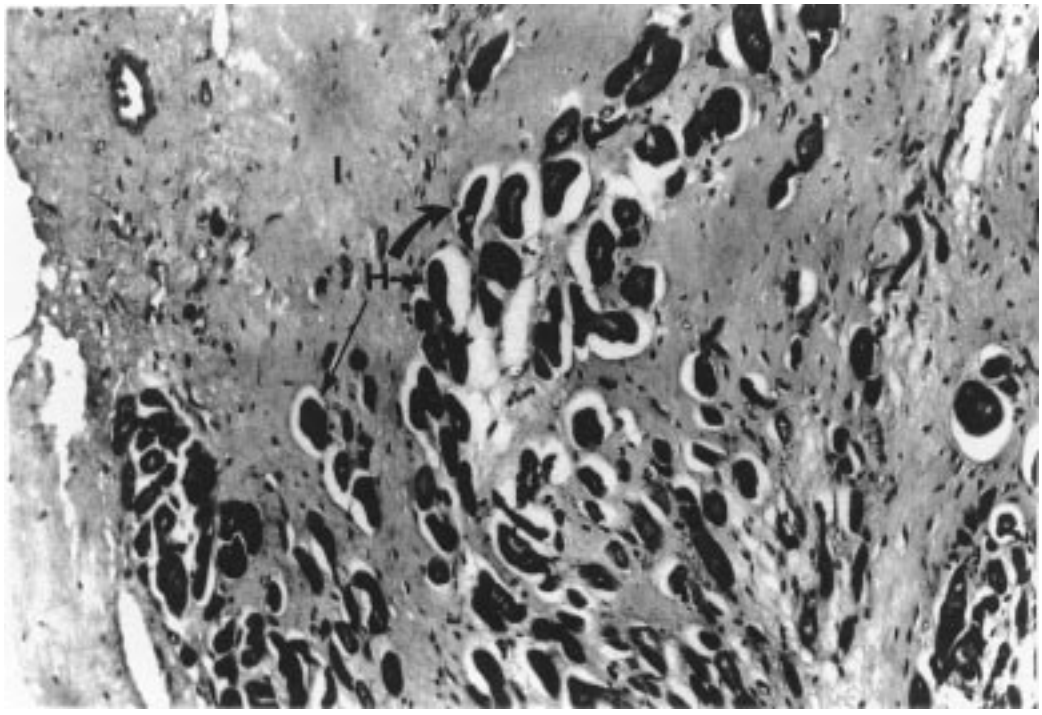

Fig. 1d. *Photomicrograph of the infarction border zone. Groups of myocytes (H) are shown interdigitating with collagen fibrils (I).*

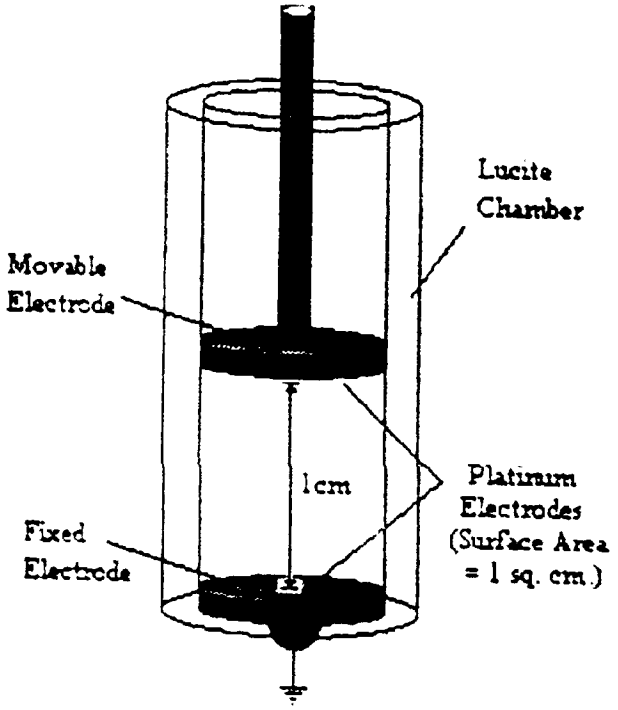

Fig. 2. *Schematic of the capacitor cell. See text for details.*

voltage to current is proportional to the tissue impedance. Measurement frequencies ranged from 1 to 40 kHz (see below). The chief advantage of the technique was that accurate measurements could be obtained over a range of frequencies by minimizing electrode artifacts such as polarization [9].

3. Unipolar. A coin-shaped platinum ("disc") electrode mounted on a catheter was utilized to perform these measurements (Fig. 4). This electrode had a diameter of 2.3 mm and a length of 0.25 mm. When oriented perpendicular to myocardium, more than 90% of the electrode surface area was in contact with myocardium; the goal of this design was to exclude simultaneous contact of a significant portion of the electrode surface area with blood. Contact with blood would have provided a parallel current path, obscuring the endocardial impedance value. Impedance was measured between the disc electrode and a cutaneous ground plate using an impedance analyzer. A single measurement frequency of 550 kHz was utilized.

Measurements in vitro and histologic analysis

Hearts were excised immediately after animals were euthanized. The left ventricle was incised along its lateral free wall, opened and mounted on a base plate. The preparation was immersed in an isotonic saline-dextrose mixture whose resistivity had been adjusted to that of whole blood (178 ohm-centimeters). On gross visual inspection, densely infarcted endocardium was sharply demarcated from healthy endocardium (Fig. 1b). We defined the infarction border in this preparation as the site of visual transition between densely infarcted and healthy endocardium. Using the border as the central zone and tracing its contour, a series of 9 isocontour zones each 2 millimeters in width were defined (hand drawn; Fig. 5). Impedance measurements were performed during a period ranging from 2 to 4 hours after resection of the heart.

Within each zone, 15 equally spaced impedance measurements around the perimeter of the infarct were performed using the four electrode technique at frequencies of 1, 5, 10, 20 and 40 kHz. At each measurement site, the probe was oriented so that the electrodes were aligned perpendicular to the infarction border contour.

To correlate tissue histology with impedance measurements, several subendocardial sections at depths $\leq$1.5 mm (the penetration range of the probe electrodes) from each endocardial isocontour zone were excised and fixed in 10% neutral buffered formalin. Each specimen was embedded in paraffin and sec-

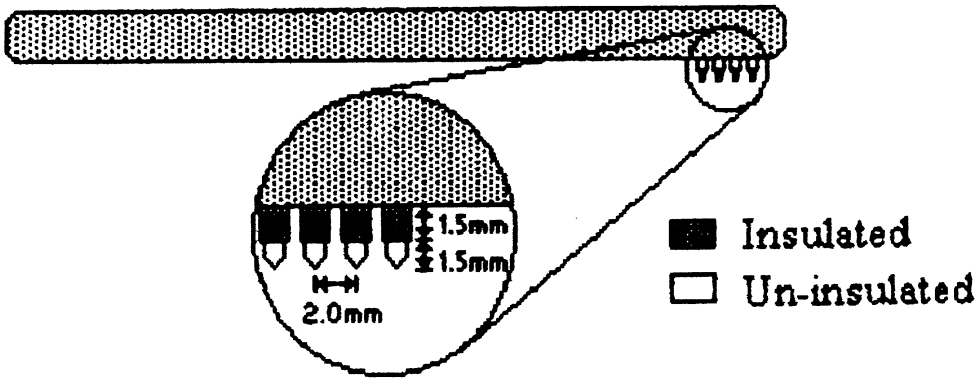

Fig. 3. *Schematic of the four-electrode probe. See text for details.*

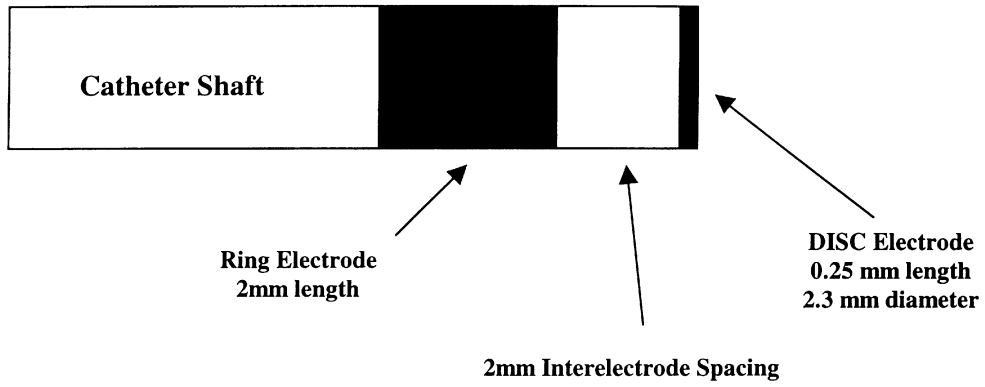

Fig. 4. Schematic of the DISC electrode. See text for details.

tioned into 5 micrometer thick layers. Specimens were stained with Richardson's modification and a combination of Verhoeff's elastic and Gomori trichrome stains. This method allowed us to visualized four different tissue types: (1) myocytes; (2) neurovascular structures; (3) collagen; and (4) elastin. Histologic examination on each specimen was then performed using a 100-block grid ocular lens at 10× magnification. Each block of the grid had an area of 0.58 square millimeters. For each specimen, the contents of 10 blocks which were felt to be representative of the entire grid were utilized for tissue content quantitation. Results were expressed as percent of each tissue type. In each animal, the tissue contents assayed from the infact zone were normalized to contents from sections of healthy myocardium obtained from a healthy area of the posterolateral ventricle, distant from the infarct. This permitted compilation of results from different animals.

Epicardial measurements in vivo

Animals were anesthetized as described above. The anterior epicardial surface of the beating left ventricle was exposed via a midline sternotomy. The heart was suspended in a pericardial cradle. Adherent pericardium and epicardial fat were carefully dissected away. On gross visual inspection, densely infarcted epicardium was sharply demarcated from healthy epicardium (Fig. 1a). We defined the infarction border in this preparation as the site of visual transition between densely infarcted and healthy epicardium. Impedance measurements were performed using the four electrode and unipolar techniques in visually

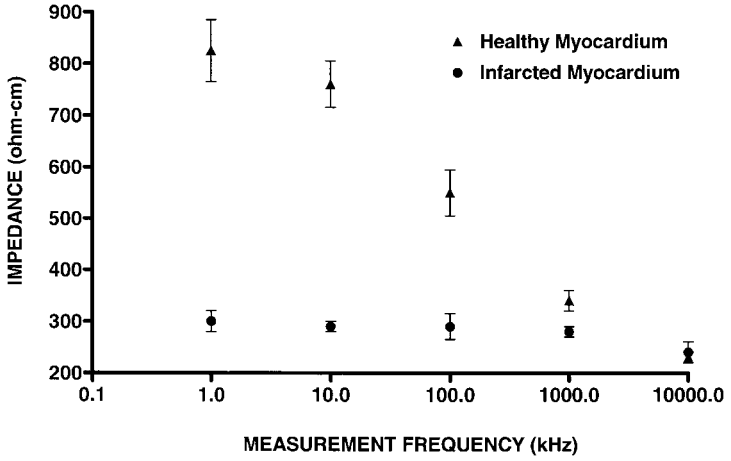

Fig. 5. Impedance measurements using the capacitor cell. Data for healthy (H) and densely infarcted (I) myocardium are presented separately. Values are mean, and represent a compilation of data from the 6 hearts in which this protocol was performed (30 specimens each for healthy and infarcted myocardium). Impedance values were obtained over a measurement frequency range of 1 kHz to 13 MHz, with ≥5 points obtained per frequency decade. Impedance values are shown at selected measurement frequencies to maximize clarity; the distributions for both healthy and infarcted myocardium were smooth and continuous and conformed to the outlines shown by the selected frequencies.

defined sites of densely infarcted, border, and healthy myocardium. At each measurement site, the four-electrode probe was oriented approximately perpendicular to the infarction border contour, and measurements were made at a frequency of 1 kHz. Unipolar impedance measurements were made at 550 kHz, using a cutaneous subscapular patch as the ground electrode.

At each measurement site, bipolar electrograms were obtained during sinus rhythm using the 2 inner electrodes of the four-electrode probe. Electrograms were recorded using both fixed (1 mV/cm) and variable gain amplification, filtered at 40–500 Hz, and recorded at a paper speed of 100 mm/sec. Electrographic peak-peak amplitude (A), duration (D) and amplitude/duration ratio (A/D) were measured for each electrogram, as described previously [10].

Endocardial measurements in vivo

A deflectable 7F catheter with the disc electrode distal and a 2 mm length proximal electrode (edge-to-edge interelectrode spacing 5 mm) was inserted percutaneously via the right femoral artery into the left ventricle using a retrograde transaortic approach in closed chest animals. Using multiplane fluoroscopy, the catheter was manipulated into approximately perpendicular contact (investigator visual estimate) with endocardium at each of 12 predesignated sites representing a random sampling of the entirety of the left ventricular endocardium using the mapping scheme described by Josephson et al. [11], as well as several additional, spatially separate sites in the region of the infarction. With respect to the latter sites, we sought that each site was at least 1 square centimeter (magnified fluoroscopic estimate) apart. This resulted in a variable number of additional sites among the cohort, ranging from 2 to 7 (see below). At each site, impedance was measured at 550 kHz, while the heart was in sinus rhythm, throughout the cardiac cycle for 60 seconds. A mean impedance value from the entire 60 second acquisition was measured. The ground electrode was a cutaneous patch located on the skin overlying the left scapula. At each measurement site, bipolar electrograms were obtained during sinus rhythm using the disc catheter (disc electrode to ring electrode, Fig. 4). Electrograms were recorded using both fixed (1 mV/cm) and variable gain amplification, filtered at 40–500 Hz, and recorded at a paper speed of 100 mm/sec. Electrographic peak-peak amplitude (A), duration (D) and amplitude/duration ratio (A/D) were measured for each electrogram, as described previously [10].

In the intact, beating heart, there was no direct visual means for assessing whether the electrode was in contact with infarcted or healthy endocardium. Pacing thresholds were not assessed. Instead, we utilized electrographic criteria as a surrogate. This technique has been previously reported in man; our epicardial electrogram data further supported its use in the ovine model [10]. In order to establish criteria for "normal" electrograms, 3 healthy sheep were studied. Bipolar sinus rhythm electrograms were recorded from the disc electrode catheter, which had been inserted percutaneously via the right femoral artery. Electrograms were recorded from each of 12 predesignated Josephson sites, and mean values ($\pm$ standard deviation) for A (7.5 $\pm$ 2.9 mV), D (36 $\pm$ 6 msec) and A/D (0.217 $\pm$ 0.092) were measured. An "abnormal" (e.g., infarcted) site was then defined separately for A, D and A/D as that which exceeded two standard deviations from the mean value: A $<$ 1.7 mV, D $>$ 48 msec, or A/D $<$ 0.033. These values were utilized in the analysis of data obtained from the chronically infarcted animals.

Units of measurement

For simplicity, we express the results of all measurement techniques as *impedance.* However, the techniques utilized in our experiments are not equivalent, in that they measure tissue properties over somewhat different volumes. The capacitor cell measures the composite impedance of the volume of tissue between its electrodes. The four-electrode technique measures impedance of the tissue in a relatively localized region between the 2 center electrodes of the measuring array. The unipolar technique measures impedance of tissue between the measuring electrode and the ground electrode; however, for practical purposes the impedance measured using this technique reflects primarily the properties of tissue within 1 millimeter of the measuring electrode [12].

Analytical methods

Results are expressed as mean $\pm$ standard deviation, unless otherwise stated. Continuous variables were compared using a t-test or an analysis of variance (Bonferroni), where appropriate. Correlation coefficients were calculated using the Spearman technique. For each statistical test, a p value of <0.05 was considered significant.

Results

Capacitor cell measurements

Six infarcted hearts were studied. In each animal, five specimens each from healthy and densely infarcted areas of the left ventricle were analyzed. Results from separate specimens in individual animals did not differ significantly. Results from different animals also did not differ significantly. Therefore, all of the data were combined to form a single distribution (Fig. 5). Impedance of healthy myocardium was comparable to previous reports [13]. Impedance was significantly greater in healthy than in infarcted myocardium at measurement frequencies below 2 MHz. The magnitude of the difference was greatest at the lowest measurement frequency, 1 kHz. In healthy myocardium, there was an

inverse relationship between impedance and measurement frequency. In infarcted myocardium, there was no significant change in impedance with measurement frequency.

Endocardial impedance measurements in vitro and histologic analysis

Three infarcted hearts were studied. Results from different animals were not significantly different, and thus these data were combined. Traversing each specimen from healthy endocardial measurement zones at greatest distance from the infarct toward the center of the infarct (Fig. 6), impedance decreased progressively (Table 1). The magnitude of the change in impedance was greatest between the border and its adjacent zones. Although significant changes were observed at each measurement frequency, the magnitude of the change in impedance was most pronounced at 1 kHz.

Traversing each specimen from healthy endocardial measurement zones at greatest distance from the infarct toward the center of the infarct (Fig. 5), tissue myocyte content decreased progressively (Fig. 7). The myocytes were replaced largely by collagen. Although the content of elastin was also significantly increased in infarcted myocardium relative to healthy myocardium, the magnitude of the increase was small relative to collagen content. There was a highly significant correlation between impedance and collagen content ($r \geq -.90$ for each measurement frequency, $p < .05$) and between impedance and myocyte content ($r \geq .90$ for each measurement frequency, $p < .05$).

Epicardial impedance measurements in vivo

Four-electrode technique. Measurements were made in 4 infarcted animals. There were no significant differences between individual animals, and thus these data were combined. Impedance in healthy epicardium was significantly greater than impedance in infarcted epicardium (Table 2). Impedance at the infarction border was intermediate between healthy and infarcted epicardium. Impedance was significantly correlated with electrogram amplitude ($r > .80$, $p < .05$), duration ($r > -.80$, $p < .05$) and amplitude/duration ratio ($r > .80$, $p < .05$) (Table 3).

Epicardial impedance was significantly lower than in endocardium *in vitro*, both in infarcted and healthy areas (Tables 1 and 2). However, the difference between epicardial and endocardial impedance was significantly greater in healthy myocardium (mean difference 430 ohms at 1 kHz, a decrease of 49% for epicardium versus endocardium, $p < .05$) than at the infarction border (mean difference 45 ohms, a decrease of 11%, $p < .05$) or in densely infarcted areas (mean difference 65 ohms, a decrease of 29%, $p < .05$).

Unipolar technique. Measurements were made in 4 infarcted animals. There were no significant differences between individual animals, and thus these data were combined. Impedance in healthy epicardium was significantly greater than impedance in infarcted epicardium (Table 2). Impedance at the infarction border was intermediate between healthy and infarcted epicardium. Impedance was significantly correlated with electrogram amplitude ($r > .80$, $p < .05$), duration ($r >$

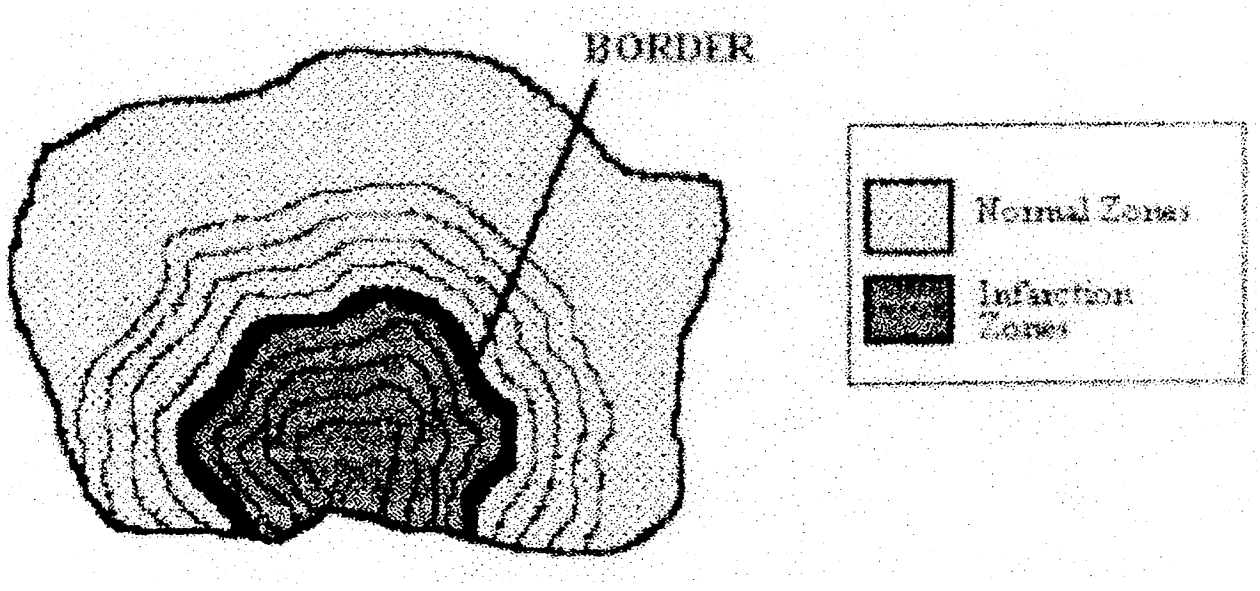

Fig. 6. *Schematic of the isocontour zones utilized for endocardial impedance measurements in vitro. The infarct morphology is similar to that shown in Figure 1b. See text for details.*

Table 1. *Impedance values (ohm-cm) from endocardial measurements performed in vitro. Values are separated by columns (the measurement zones relative to the infarction border, as diagrammed in Figure 5 ranging from healthy myocardium [left] to densely infarcted myocardium [right]), and rows (the frequencies at which impedance was measured). Values are mean ± standard deviation for the compilation of date from all 3 animals in which this protocol was performed (n = 45 measurements). ANOVA p < .05 for each frequency. B = infarction border zone.*

	Healthy → Infarcted								
	8mm	6mm	4mm	2mm	B.	2mm	4mm	6mm	8mm
1 kHz	878 ± 214	809 ± 222	778 ± 233	644 ± 216	425 ± 174	275 ± 88	229 ± 60	229 ± 40	225 ± 28
5 kHz	823 ± 176	765 ± 182	737 ± 192	621 ± 186	423 ± 166	292 ± 96	244 ± 64	244 ± 50	230 ± 29
10 kHz	801 ± 158	749 ± 163	721 ± 176	609 ± 191	443 ± 179	308 ± 108	256 ± 64	263 ± 64	231 ± 31
20 kHz	783 ± 144	739 ± 153	726 ± 169	633 ± 174	456 ± 172	327 ± 121	274 ± 76	286 ± 74	245 ± 32
40 kHz	728 ± 176	684 ± 173	689 ± 209	583 ± 182	428 ± 176	317 ± 136	265 ± 70	274 ± 52	248 ± 30

−.80, p < .05) and amplitude/duration ratio (r > .80, p < .05) (Table 3).

Endocardial impedance measurements in vivo

Impedance measurements were performed in 3 infarcted animals. In each animal, the mean impedance at sites with abnormal electrograms (defined above) was significantly lower than at sites with normal electrograms (Table 4). Figure 8 shows the individual impedance values obtained from each of the three animals. For each animal, impedance values are separated into those obtained at sites where normal electrograms were recorded and those obtained at sites where abnormal electrograms were recorded. Impedance at normal electrogram sites was significantly greater than impedance at abnormal electrogram sites. In two of the three animals, the lowest impedance value obtained from normal electrogram sites was still greater than the highest impedance value obtained from abnormal electrogram sites.

Discussion

The bulk electrical properties of myocardium have long been studied [8,9,14–16]. Published data have var-

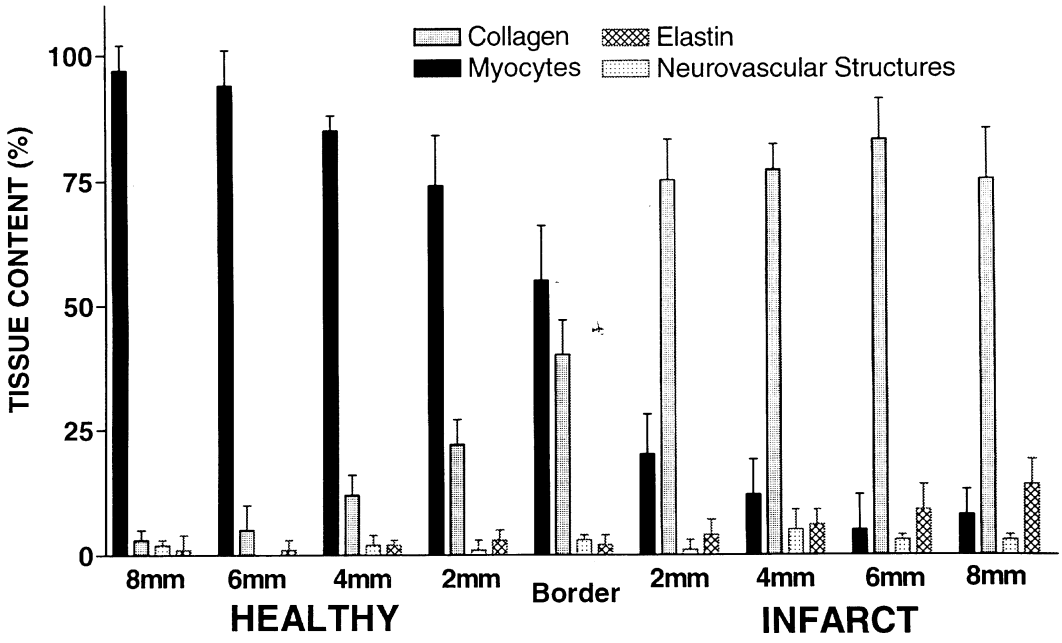

Fig. 7. *Histological analysis results. The ordinate shows the quantitative content of each tissue (myocytes, collagen, elastin, and neurovascular elements) as a percentage. The abscissa separates the data by isocontour zones utilized for endocardial impedance measurements in vitro (Fig. 5; H = healthy myocardium, I = infarcted myocardium, B = infarction border). Contents are the mean of a compilation of values from the 3 hearts in which this protocol was performed (≥9 specimens per isocontour zone). ANOVA p < .05 for myocytes, collagen, and elastin.*

Table 2. *Impedance values (units are ohms-cm for four-electrode technique and ohms for unipolar technique) from epicardial measurements performed in vivo. Values are separated by columns (the measurement zones as defined visually as dense infarction, infarction border, and healthy myocardium) and rows (the impedance measurement technique). Measurement frequency was 1 kHz for four-electrode technique and 550 kHz for unipolar technique. Values are mean ± standard deviation for the compilation of data from all 4 animals in which this protocol was performed. Units for four-electrode technique are ohms-cm, and for unipolar technique are ohms. ANOVA $p < .05$ for each impedance measurement technique.*

	Healthy (n = 36 sites)	Border (n = 28 sites)	Densely infarcted (n = 40 sites)
Four-electrode	450 ± 90	380 ± 60	160 ± 30
Unipolar	345 ± 15	280 ± 20	240 ± 10

ied markedly with both measurement technique and tissue preparation. Recent work has focused on the ability of impedance to detect myocardial ischemia. For example, in dogs following coronary ligation, Ellenby et.al. observed an abrupt rise in left ventricular *epicardial* impedance within minutes after onset of infarction, which was maximal by one hour [4]. Until recently, there were no reports addressing the impedance properties of chronically infarcted myocardium. Fallert et al. showed that *epicardial* impedance in chronically (6 weeks) infarcted sheep was markedly lower than at baseline [3]. These investigators utilized the four-electrode technique and measured impedance at frequencies of 1, 5 and 15 kHz. However, they did not perform endocardial measurements, nor did they assess tissue near the infarction border zone. In addition, they did not correlate electrogram features or tissue histology with impedance. Our results thus extend this data. We confirmed that marked differences in impedance exist between healthy and chronically infarcted myocardium. Impedance in healthy myocardium also had a marked frequency dependence, which was not observed in infarcted myocardium. These differences are likely due to pronounced differences in intact cell (membrane) volume fraction between healthy and densely infarcted myocardium, greater in the former. As demonstrated in our histologic analysis, in healthy myocardium myocytes dominate the tissue content, whereas in densely infarcted myocardium the major component of the tissue content is collagen. A greater cell volume fraction imparts both higher impedance and a stronger frequency dependence to its measurement. A theoretical explanation for our observations utilizing tissue electrical property theory can be proposed [16]. There are two potential current pathways through a tissue, through the cells (intracellular) and through the interstitial space (extracellular). The total impedance of a tissue is thus a combination of impedance of the two current paths. Cell membranes appear to behave as capacitors in that their impedance has an inverse relationship with frequency. Thus, at low frequencies cells are essentially non-conductive, whereas at high frequencies their conductivity approaches that of cytoplasm and the interstitial space). As shown by our histologic analysis, densely infarcted myocardium is largely acellular. Thus, current predominantly flows in an extracellular matrix, whose impedance is not frequency dependent, at least in the frequency range which we assessed. In healthy myocardium, the volume fraction of intact cells is relatively high and the impedance of the extracellular pathway is also high (since there is little of it to conduct current). Consequently, the bulk tissue impedance is relatively high and is also frequency dependent, since it is determined largely by the impedance properties of the cell membranes. The intermediate impedance properties of the infarction border zone, associated with intermediate myocyte content, add further support to the concept of the myocyte membrane as the underlying reason for impedance frequency-dependence.

Our *in vivo* analysis of both epicardial and endocardial ventricular impedance confirms that there is a significant difference in impedance between healthy and chronically infarcted myocardium, with the infarction border zone having an intermediate value. Electrogram amplitude was directly associated with impedance, whereas electrogram duration manifested an inverse relationship.

We observed that impedance was lower in epicardium *in vivo* than in the endocardium *in vitro*. This was likely due to a change in the tissue electrical prop-

Table 3. *Sinus rhythm electrogram values from epicardial measurements performed in vivo. Values are separated by columns (bipolar electrogram amplitude [millivolts], duration [milliseconds], and amplitude/duration ratio [millivolts/millisecond]) and rows (visually defined regions, including healthy and densely infarcted areas, as well as infarction border. n = number of separate measurement sites). Values are mean ± standard deviation for the compilation of data from all 4 animals in which this protocol was performed. ANOVA $p < .05$ for each of amplitude, duration and amplitude/duration ratio comparisons between regions.*

	Amplitude (mV)	Duration (msec)	A/D (mV/msec)
Healthy (n = 36)	5.8 ± 1.2	34 ± 5	0.17 ± 0.02
Infarct Border (n = 28)	1.8 ± 1.2	42 ± 2	0.04 ± 0.006
Dense Infarct (n = 40)	1.2 ± 0.2	58 ± 2	0.02 ± 0.001

Table 4. *Endocardial impedance values (ohms) acquired in vivo. Values are separated by columns (electrographically normal versus electrographically abnormal sites) and rows (the specific electrogram feature used to define whether the electrogram was normal or abnormal: 1. electrogram amplitude; 2. electrogram duration; or 3. electrogram amplitude/duration ratio. See text for details). Measurement frequency was 550 kHz. Values are mean ± standard deviation for the compilation of data from all 3 animals in which this protocol was performed.*

	Egm normal sites	Egm abnormal sites	P
EGM feature			
Amplitude	245 ± 30 (n = 45)	191 ± 31 (n = 18)	.001
Duration	243 ± 49 (n = 43)	204 ± 44 (n = 20)	.01
A:D Ratio	244 ± 48 (n = 49)	183 ± 33 (n = 14)	<.001

erties of the *in vitro* preparation induced by anoxia which occurred after extirpation. With an anoxic insult, both myocyte swelling and cell-to-cell uncoupling occur [3,4,17,18]. Cell swelling would result in a decrease in interstitial volume, likely causing an increase in extracellular impedance. Cell-to-cell uncoupling would increase intracellular longitudinal resistance. These changes would collaborate to cause an increase in tissue impedance, due solely to the anoxic insult [3]. The observation that the difference in impedance between *in vivo* and *in vitro* preparations in infarcted or border tissue was presumably due to the reduced myocyte content in these zones.

Our results also suggest that endocardial impedance can be measured effectively using an electrode catheter inserted percutaneously into a beating heart. We temper this conclusion due to the lack of correlative tissue histology, as well as the lack of an adequate assessment of electrode-endocardial contact in these experiments. With regard to the latter, we note that for both electrographically normal and abnormal sites, endocardial impedance *in vivo* was generally lower than *in vitro*, despite the use of the same measurement technique. We ascribe this to differences in the current path for open chest versus closed chest unipolar measurements. For example, during endocardial impedance measurement *in vivo*, some degree of cavitary blood-electrode was inevitable. Whole blood has a significantly lower impedance than either healthy or chronically infarcted myocardium [3,12].

The present study has significant limitations. First, as detailed above the tissue assessed in the *in vitro* and *in vivo* experiments was different. Tissue utilized for the *in vitro* preparations was ischemic, and this undoubtedly magnified the impedance differences between healthy and infarcted myocardium. However,

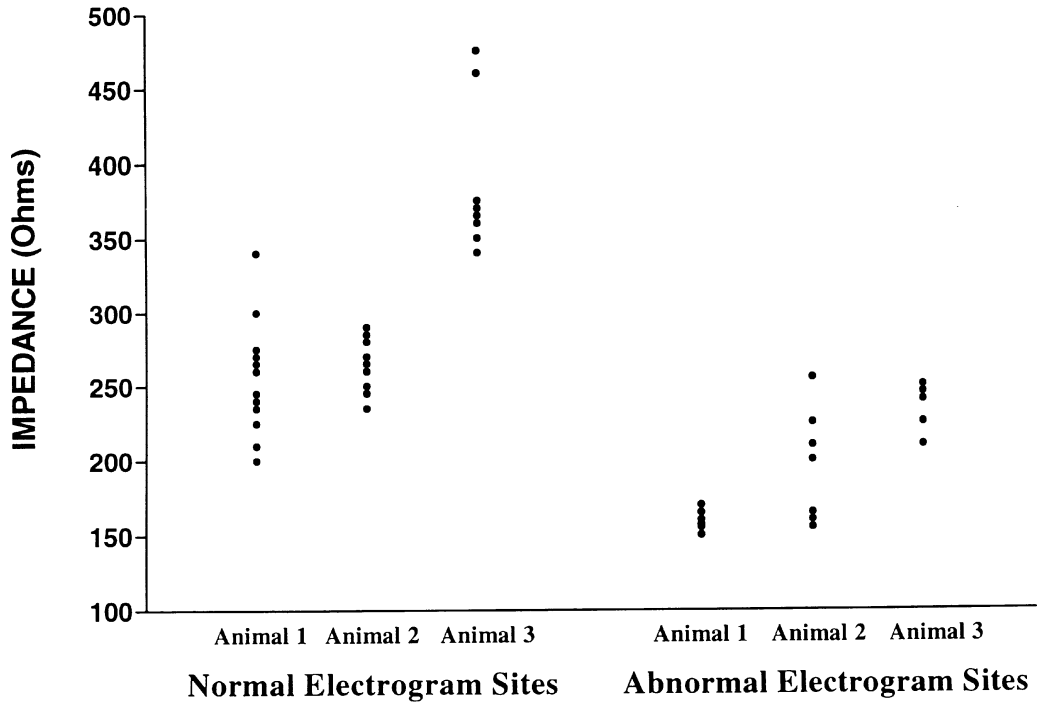

Fig. 8. *In vivo endocardial impedance measurements obtained from each of the 3 animals in which this protocol was performed. Individual impedance values are shown on the ordinate. The data are separated by individual animal on the abscissa. In addition, the data on the abscissa are separated by whether the bipolar electrogram recorded was normal or abnormal (see text). For this figure, an abnormal electrogram was defined as abnormality of amplitude and/or duration and/or amplitude/duration ratio.*

our goal for the *in vitro* experiments was not to obtain impedance values accurate for measurement *in vivo*, rather to permit spatially detailed measurement on the endocardium to be correlated with tissue histology; this would not have been possible *in vivo*. The experiments *in vivo* established that impedance differences were not artifactual. Second, myocardial impedance is clearly anisotropic [3,9]. In the present study, we made no effort to identify fiber orientation or measure the degree of variation in impedance with electrode orientation. However, the interelectrode spacing on our four-electrode probe was wide compared to fiber length, and thus we would anticipate the influence of anisotropy to be small. Furthermore, we would expect anisotropy to be far less pronounced in infarcted myocardium, as the effect is related to the presence of myocytes [3].

Potential for utility as a cardiac mapping technique

These data demonstrate that myocardial impedance provides insight into local cardiac tissue content. They may provide the basis for further investigation of the utility of electrical impedance as a tool for assessing cardiac tissue. We were particularly interested in utilizing impedance to locate areas of ventricular tissue which might support electrical reentry, frequently located at infarction border zones [1,2,19]. Although our data do not address this issue, it is conceivable that ventricular tissue with the potential to support reentrant circuits might have a finite range of myocyte content. Unlike electrographic data, impedance values should not be susceptible to functional variation [19]. However, based on the local nature of the impedance measurement, electrode designs would likely have to include those which could be inserted intramurally, depending on infarct location. For endocardial mapping, barriers preventing direct electrode access to endocardium (e.g., endocavitary thrombus), or electrode design flaws which allow simultaneous cavitary blood access to the electrode(s) surface would have to be overcome.

References

1. Bolick DR, Hackel DB, Reimer KA. Quantitative analysis of myocardial infarct structure in patients with ventricular tachycardia. *Circulation* 1986;74(6):1266–1279.
2. Gardner PI, Ursell, PC, Fenoglio JJ, Wit AL. Electrophysiologic and anatomic basis for fractionated electrograms recorded from healed myocardial infarcts. *Circulation* 1985;72:596–605.
3. Fallert MA, Mirotznik MS, Downing SW, Savage EB, Foster KR, Josephson ME, Bogen DK. Myocardial electrical impedance mapping of ischemic sheep hearts and healing aneurysms. *Circulation* 1993;87:199–207.
4. Ellenby MI, Small KW, Wells RM, Hoyt DJ, Lowe JE. Online detection of reversible myocardial ischemic injury by measurement of myocardial electrical impedance. *Ann Thorac Surg* 1987;44:587–597.
5. Markovitz LJ, Savage EB, Ratcliffe MB, Bavaria JE, Kreiner G, Iozzo RV, Hargrove WC, Bogen DK, Edmunds LH Jr. Large animal model of left ventricular aneurysm. *Ann Thorac Surg* 1989;48:838–845.
6. Kreiner G, Gottlieb CD, Yeh IT, Furukawa S, Miller JM, Edmunds LH Jr, Bavaria JE, Bernstein RC, Hargrove WC, Tyson GS. Ventricular tachycardia in an ovine model of left ventricular aneurysm. *Surg Forum* 1989;40:219–223.
7. Kreiner G, Gottlieb CD, Furukawa S, Simson MB, Tyson GS, Edmunds LH Jr. Late potentials in an ovine model of transmural myocardial infarction. *J Appl Physiol* 1992;73(3): 841–845.
8. Schwan HP. Determination of biological impedances. In: *Physical Techniques in Biological Research.* Volume 6. 1963,323–407.
9. Steendijk P, Mur G, Van Der Veld ET. The four-electrode resistivity technique in anisotropic media: theoretical analysis and application on myocardial tissue *in vivo*. *IEEE Transactions on Biomedical Engineering* 1993;40(11): 1138–1147.
10. Cassidy DM, Vasallo JA, Buxton AE, Doherty JU, Marchlinski FE, Josephson ME. The value of catheter mapping during sinus rhythm to localize the site of origin of ventricular tachycardia. *Circulation* 1984;69:1103–1110.
11. Josephson ME, Horowitz LN, Marchlinski FE. The role of catheter mapping in the preoperative evaluation of ventricular tachycardia. *Am J Cardiol* 1982;49:207–215.
12. Schwan HP. Electrical properties measured with alternating currents: Body tissues. In: Spector WS Jr, ed. *Handbook of Biological Data.* Philadelphia: WB Saunders, 1956.
13. Gabriel C. The dielectric properties of biological tissues: I. Literature survey. *Phys Med Biol* 1996;41:2231–2249.
14. Surowiec A, Stuchly SS, Eidus L, Swarup A. In vitro dielectric properties of human tissues at radiofrequencies. *Phys Med Biol* 1987;32:615–621.
15. Schwan HP. Linear and nonlinear electrode polarization and biological materials. *Ann Biomed Res* 1992;20:269–288.
16. Foster KR, Schwan HP. Dielectric properties of tissues and biological materials. A critical review. *Critical Reviews in Biomedical Engineering* 1989;17(1):25–104.
17. Kleber AG, Riegger CB, Janse MJ. Electrical uncoupling and increase of extracellular resistance after induction of ischemia in isolated, arterially perfused rabit papillary muscle. *Circ Res* 1987;61:271–279.
18. Cinca J, Warren M, Carreno A, Tresanchez M, Armadans L, Gomez P, Soler-Soler J. Changes in myocardial electrical impedance induced by coronary artery occlusion in pigs with and without preconditioning. *Circ Res* 1997;96 3079–3086.
19. DeBakker JMT, Van Capelle FJL, Janse MJ, Wilde AAM, Coronel R, Becker AE, Dingemans KP, Van Hemel NM, Hauer RNW. Reentry as a cause of ventricular tachycardia in patients with chronic ischemic heart disease: Electrophysiologic and anatomic correlation. *Circulation* 1988; 77(3):589–600.